Steel and Composite Structures, *Vol. 17, No. 6 (2014) 929-949*
DOI: http://dx.doi.org/10.12989/scs.2014.17.6.929

Bond behaviors of shape steel embedded in recycled aggregate concrete and recycled aggregate concrete filled in steel tubes

Zongping Chen [*1,2], Jinjun Xu [1a], Ying Liang [1] and Yisheng Su [1]

[1] *College of Civil Engineering and Architecture, Guangxi University, Nanning, 530004, P.R. China*
[2] *Key Laboratory of Disaster Prevention and Structural Safety of Chinese Education Ministry, Guangxi University, Nanning, 530004, P.R. China*

(*Received September 25, 2013, Revised March 25, 2014, Accepted April 23, 2014*)

Abstract. Thirty one push-out tests were carried out in order to investigate the bond behavior between shape steel, steel tube (named steels) and recycled aggregate concrete (RAC), including 11 steel reinforced recycled aggregate concrete (SRRAC) columns, 10 recycled aggregate concrete-filled circular steel tube (RACFCST) columns and 10 recycled aggregate concrete-filled square steel tube (RACFSST) columns. Eleven recycled coarse aggregate (RCA) replacement ratios (i.e., 0%, 10%, 20%, 30%, 40%, 50%, 60%, 70%, 80%, 90% and 100%) were considered for SRRAC specimens, while five RCA replacement ratios (i.e., 0%, 25%, 50%, 75% and 100%), concrete type and length-diameter ratio for recycled aggregate concrete-filled steel tube (RACFST) specimens were designed in this paper. Based on the test results, the influences of all variable parameters on the bond strength between steels and RAC were investigated. It was found that the load-slip curves at the loading end appeared the initial slip earlier than the curves at the free end. In addition, eight practical bond strength models were applied to make checking computations for all the specimens. The theoretical analytical model for interfacial bond shear transmission length in each type of steel-RAC composite columns was established through the mechanical derivation, which can be used to design and evaluate the performance of anchorage zones in steel-RAC composite structures.

Keywords: recycled aggregate concrete (RAC); shape steel; steel tube; bond mechanism; transmission length

1. Introduction

Wenchuan earthquake (May 12, 2008) in China (Zhao *et al*. 2009, Michael and Li 2011) and the Fukushima earthquake in Japan (March 11, 2011) (Liu *et al*. 2011, Takewaki *et al*. 2011, Nandasena *et al*. 2012), caused thousands of houses collapsed and/or destroyed, which produced plenty of waste concrete and led to serious harm to the ecological environment. Therefore, it has been a major issue for all the countries suffered from natural disasters - how to rebuild their homes and how to reasonably and scientifically deal with these building garbage. Governments have

*Corresponding author, Ph.D., E-mail: zpchen@gxu.edu.cn
[a] Ph.D. Student, E-mail: jjxu_concrete@163.com

http://www.techno-press.org/?journal=scs&subpage=8 ISSN: 1229-9367 (Print), 1598-6233 (Online)

introduced different kinds of policies to speed up the waste concrete recycling and energy-saving building development process. The use of recycled aggregate concrete (RAC) is one such an attempt and is one way to solve some of the problems in construction engineering.

Steel-RAC composite structures refer to the structures composed of shape steel or steel tube and RAC. It combines the advantages of traditional composite structures (i.e., high bearing capacity and good seismic performance) and the benefits of using RAC materials. In fact, large amount of experimental work has been carried out in the past. For the RAC material research, most of findings have been extensively reviewed and discussed by Nixon (1978), Hansen (1992) and Xiao *et al*. (2005). While for the steel-RAC structure research, some study works have been launched in the field of steel reinforced recycled aggregate concrete (SRRAC) and recycled aggregate concrete-filled steel tube (RACFST). In the aspect of SRRAC, Qin *et al*. (2012) tested six steel reinforced recycled aggregate concrete beams to investigate their flexural performance; in addition, six steel reinforced recycled aggregate concrete composite columns were tested under axial compression by Chen *et al*. (2011), where two factors, including recycled coarse aggregate (RCA) replacement percentage and slenderness ratio of column, were taken into consideration. In another aspect, the compressive behavior of RACFST columns was explained by Konno *et al*. (1997), Yang and Han (2006), Liu *et al*. (2012) and Huang *et al*. (2012). But in fact, considering structures as a whole body, it is a fundamental issue to consider the interfacial bond behavior between steels and RAC. Up to now, it is well-known that studies on the bond behavior between natural aggregate concrete (NAC) and steel bars has arisen wide attention in the engineering world for a long time, and parts of research works also have been launched in the field of bond behavior between steel bars and RAC (Xiao and Falkner 2007, Gholamreza *et al*. 2012). However, the knowledge of bond mechanism between steels and RAC seems to be comparatively limited in the qualitative stage.

This paper considers the RAC replacement ratio, steel type, cross-section type, concrete type and length-diameter ratio as the main experimental parameters. The aim of this work is to investigate the bond behavior between steels and RAC, and to establish the bond shear transmission mechanism between steels and RAC. Push-out tests were carried out to investigate the bond strength and load-slip curves with different RAC replacement ratios. What's more, the practical bond strength calculation formulas were applied to check computations for each type of steel-RAC specimens.

2. Test program

2.1 Materials

Cement (C): Portland cement, CEM I-32.5R, with a 28d compressive strength of 32.5 MPa. Water (W): city tap water was used in this investigation. Fine aggregate (FA) was the river sand. Natural coarse aggregate (NCA) were graded with continuous distributions and their maximum grain size was 20 mm. Recycled coarse aggregate (RCA) was obtained from the waste reinforced concrete (RC) poles in a line of China Southern Power Grid, which has been in service over 50 years. The original design compressive strength of these RC poles was C30 (31 MPa measured). The size fraction used was 4-20 mm (4-20 R) with continuous distributions. All coarse aggregate were washed for several times and dried out naturally.

Hot rolled H-shaped steel, deformed low carbon steel bars (HRB335) and plain low carbon steel

Table 1 Mechanical properties of steels

Steel form	f_y (MPa)	f_u (MPa)	E_s (MPa)
HRB335, Φ16	376.90	571.90	2.231×10^5
HPB235	271.40	430.60	2.217×10^5
Steel web in the H-shaped steel	312.20	391.50	2.213×10^5
Steel flange in the H-shaped steel	328.40	461.50	2.126×10^5
Φ140×3 of circular tube	345.90	455.60	2.033×10^5
120×120 of square tube	303.27	394.09	1.926×10^5

*Note: f_y is the yield strength; f_u is the ultimate strength; E_s is the modulus of elasticity

Table 2 Mix proportions of concrete (kg/m^3)

Concrete type	Cement	Water	Fine aggregate	Coarse aggregate
C30	500.0	205.0	525.0	1170.0
C50	641.5	205.0	590.0	963.5

bars (HPB235) were used for SRRAC specimens; circular steel tubes with external diameter of 140 mm and wall thickness of 3 mm for RACFCST were used in the tests; square steel tubes with side length of 120 mm and wall thickness of 3 mm were adopted for RACFSST. The mechanical properties of steels were tested according to the Chinese standard GB/T 228-2002, and they are listed in Table 1.

2.2 Mix proportion

The ratio of RCA to the total coarse aggregate by weight is the term of RCA replacement ratio (δ). The design is consisted of three batches of steel-RAC composite columns: (a) eleven types of steel reinforced recycled aggregate concrete specimens were fabricated with the replacement ratio δ of 0%, 10%, 20%, 30%, 40%, 50%, 60%, 70%, 80%, 90% and 100% of RCA, respectively; (b) ten recycled aggregate concrete-filled circular steel tube specimens were manufactured with the replacement ratio δ of 0%, 25%, 50%, 75%, and 100% of RCA in each group; (c) ten recycled aggregate concrete-filled square steel tube specimens were manufactured with the replacement ratio δ of 0%, 25%, 50%, 75%, and 100% of RCA in each group. In this test, RAC with different replacement ratios were strictly kept the same in following aspects: cement, water and sand. The only variable was the attribute of coarse aggregate. That is to say that NCA reduced along with the increase of RCA accordingly. The concrete strength configuration was acquired based on the RCA replacement ratio of 0%, and there were two types of concrete in this study, where the test strengths designed were C30 (low-strength RAC: LSRAC) and C50 (high-strength RAC: HSRAC) for RACFSST.

In fact, the greatest distinctive feature of RCA compared to NCA is their higher water absorption capacity, due mainly to adhered mortar (Nixon 1978, De Juan and Gutiérrez 2009). This adhered mortar is also called old cement mortar substrate. In other words, additional absorbing moisture of RCA from the air can have a curing effect on the concrete strength. Based on the above considerations, the design water-cement (W/C) ratios were kept constant for each concrete type in order to focus only on the influence of water absorption capacity of RAC on bond

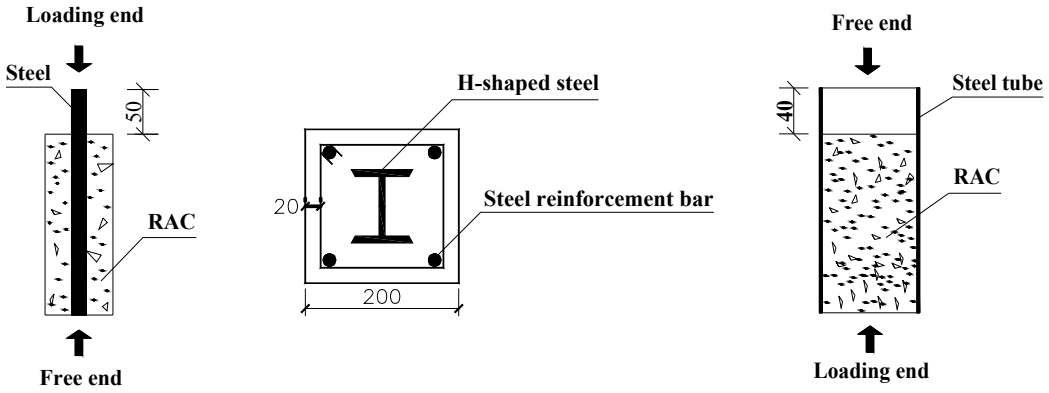

(a) SRRAC (b) RACFST

Fig. 1 Sketch of push-out specimens (unit: mm)

mechanical property. The mix proportions of concrete are shown in Table 2.

2.3 Preparation of specimens

Fig. 1 shows the sketch of push-out test specimens. The main information about the specimens is given in Table 3. The specimens were cast with the steel in a vertical position in order to simulate the situation of end steel anchorage in concrete columns. The steels were rust free. For SRRAC, only one test parameter was considered, and that is the RCA replacement ratio. The thickness of concrete covering was kept constant as 50 mm. When fabricating the SRRAC specimens, the loading end was the end of shape steel extending the concrete surface with the length size of 50 mm, and the free end was the end keeping the shape steel and concrete in the same plane (shown in Fig. 1). For RACFST, the RCA replacement ratio, the concrete type and the length-diameter ratio were taken into consideration as the main experimental parameters. In addition, steel types and cross-section types in these three kinds of steel-RAC composite columns were the selling points in comparison of their bond behaviors. As shown in Fig. 1, the free end was the end of steel tube extending the concrete surface with the length size of 40 mm, and the loading end was the end keeping the steel tube and concrete in the same plane.

All of the specimens were de-moulde done day after casting and then moved to the curing room under natural conditions for 28 days. The mean values of RAC measured cube compressive strength (f_{cu}) are listed in Table 3.

2.4 Test setup

Prior to the bond test, the top and bottom surfaces of all the specimens were pure smooth to provide a level surface and to ensure evenly distribution of the applied loads. The push-out test setup is shown in Fig. 2. The RMT-201 rock and concrete mechanics test system, which is researched and developed in Wuhan Institute of Rock and Soil Mechanics, is controlled by multi-function electro-hydraulic servo tester. In the test, there is a difference which needs to be explained: the shape steel in SRRAC column was pushed out the concrete, while the core concrete filled in steel tube was pushed out oppositely. When testing SRRAC, a thick steel block was

Table 3 Description of the push-out specimens

Specimen code	Column type	Sectional dimension (mm)	δ	Concrete type	f_{cu} (MPa)	L_e (mm)	L_e/D
S-RAC-1	SRRAC	200 × 200	0%	C30	31.5	460	—
S-RAC-2		200 × 200	10%	C30	33.1	460	—
S-RAC-3		200 × 200	20%	C30	34.1	460	—
S-RAC-4		200 × 200	30%	C30	33.1	460	—
S-RAC-5		200 × 200	40%	C30	36.0	460	—
S-RAC-6		200 × 200	50%	C30	35.7	460	—
S-RAC-7		200 × 200	60%	C30	37.0	460	—
S-RAC-8		200 × 200	70%	C30	39.6	460	—
S-RAC-9		200 × 200	80%	C30	40.8	460	—
S-RAC-10		200 × 200	90%	C30	39.3	460	—
S-RAC-11		200 × 200	100	C30	38.5	460	—
S-RAC-12	RACFCST	Φ140 × 3	0%	C50	58.5	410	2.93
S-RAC-13		Φ140 × 3	25%	C50	59.2	410	2.93
S-RAC-14		Φ140 × 3	50%	C50	57.6	410	2.93
S-RAC-15		Φ140 × 3	75%	C50	56.8	410	2.93
S-RAC-16		Φ140 × 3	100%	C50	55.5	410	2.93
S-RAC-17		Φ140 × 3	0%	C50	58.5	260	1.86
S-RAC-18		Φ140 × 3	25%	C50	59.2	260	1.86
S-RAC-19		Φ140 × 3	50%	C50	57.6	260	1.86
S-RAC-20		Φ140 × 3	75%	C50	56.8	260	1.86
S-RAC-21		Φ140 × 3	100%	C50	55.5	260	1.86
S-RAC-22	RACFSST	120 × 120	25%	C50	59.2	410	3.42
S-RAC-23		120 × 120	50%	C50	57.6	410	3.42
S-RAC-24		120 × 120	75%	C50	56.8	410	3.42
S-RAC-25		120 × 120	100%	C50	55.5	410	3.42
S-RAC-26		120 × 120	0%	C50	58.5	260	2.17
S-RAC-27		120 × 120	25%	C50	59.2	260	2.17
S-RAC-28		120 × 120	50%	C50	57.6	260	2.17
S-RAC-29		120 × 120	75%	C50	56.8	260	2.17
S-RAC-30		120 × 120	100%	C50	55.5	260	2.17
S-RAC-31		120 × 120	75%	C30	40.5	260	2.17

*Note: δ is the parameter that is expressing the RCA replacement ratio; L_e is the interfacial embedded length of steel in concrete; L_e/D is used for describing the equivalent length-diameter ratio of steel tube, where $B = D$ for RACFSST

placed between the free end of specimen and the test machine. H-typed hole was dug in the middle of the steel block with slightly larger size compared with the inner H-shaped steel. While for testing RACFST, a thick steel block was placed between the loading end of specimen and the test machine. The steel block had a cross-section which was slightly smaller than that of the inside

(a) SRRAC (b) RACFST

Fig. 2 Test setup

diameter/edge of steel tube. The above measures assured the load to be applied only on the core concrete and allowed the shape steel or core concrete to be pushed out when testing.

All specimens were tested under monotonic load with the loading rate of 0.005 mm/s. The push-out load (P) and slips (s) both at the loading end and the free end of test specimens were measured in order to determine a load-slip relationship. The slips were achieved by the record of two linear variable differential transducers (LVDT) mounted on the specimen as shown in Fig. 2. One LVDT measured the movement of the shape steel extended the concrete for SRRAC or core concrete surface at the same level of steel tube for RACFST at the loading end, while the other one recorded the displacement of the free end of the steel embedded in the concrete for SRRAC or the constrained concrete with the air gap for RACFST.

3. Test results and analysis

3.1 Load-slip (P-s) curves

Fig. 3 shows the typical curves of push-out load versus slip at the loading end and the free end for these three kinds of steel-RAC composite columns. Apparently, it can be found that there are some noticeable features for load-slip curves at both ends. Through with inductive analysis, comparative results among three types of specimens are listed as follows:

- At the loading end: For SRRAC columns, there are at most five stages presented on the *P-s* curves, which are made of the non-slip section, slip ascent section, peak point, sudden plunged section and gentle decline section; for RACFCST columns, four stages make up the curves, including the non-slip section, ascent section after starting slip, peak point and descent section; while for RACFSST columns, the *P-s* curves are composed of the non-slip section, ascent section after starting slip, peak point, descent section, re-rising section, second peak point and re-descent section. In addition, it is worth noting that the second peak points are universally smaller than the first ones. In this paper, the above three kinds of curves can be named Type A, Type B and Type C, respectively.
- At the free end: Compared with *P-s* curves at the loading end for SRRAC specimens, a

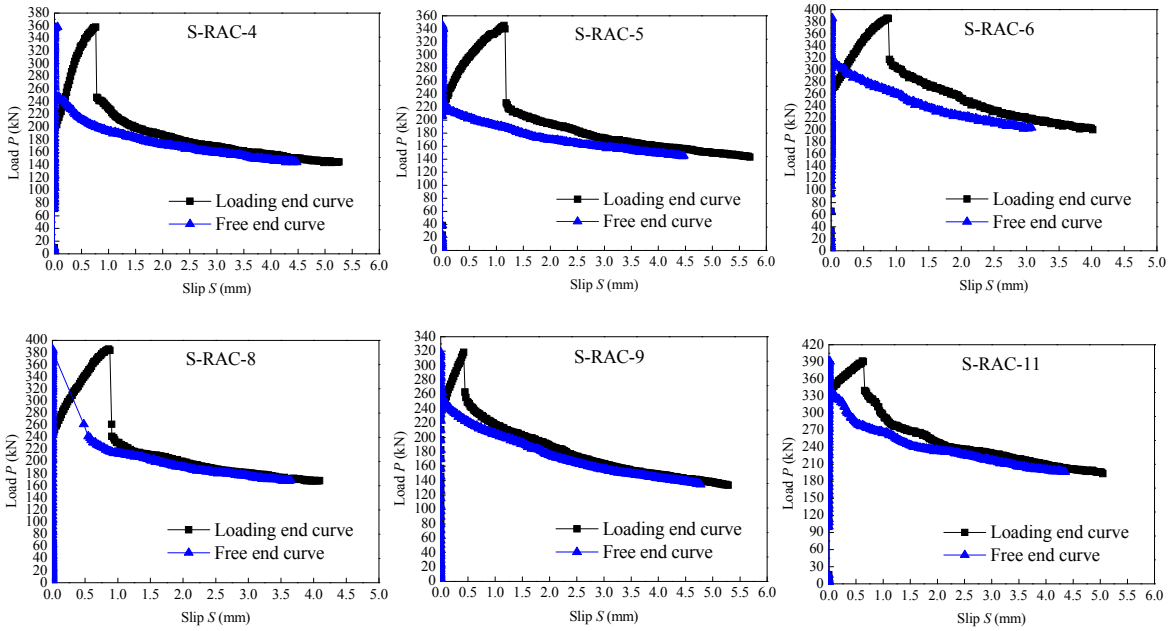

(a) SRRAC specimens

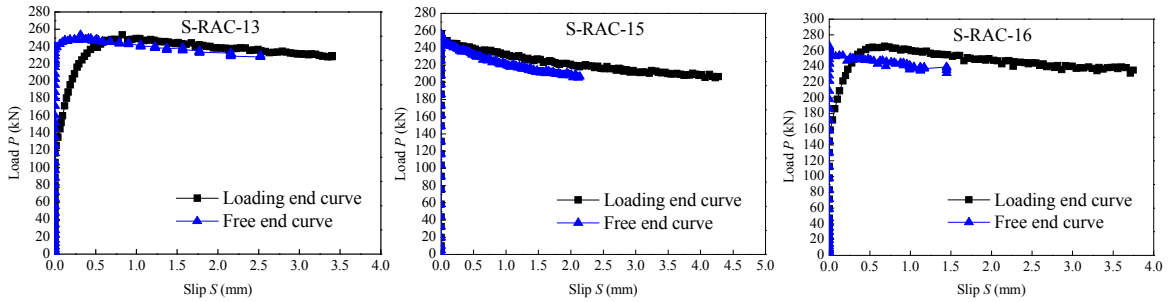

(b) Circular specimens

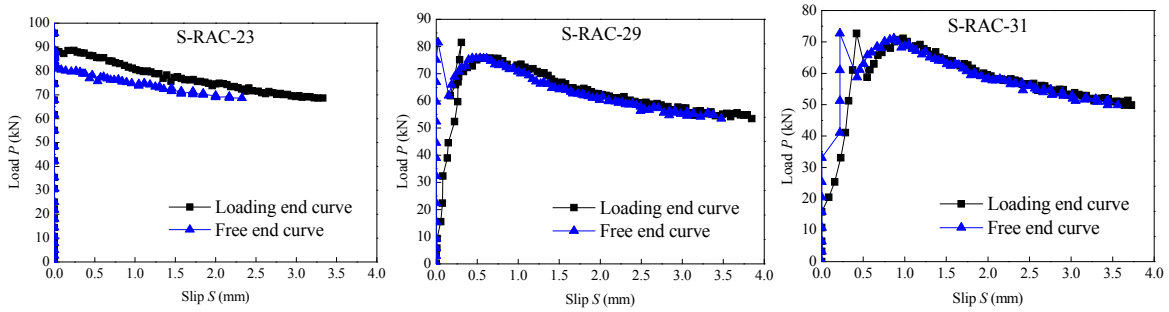

(c) Square specimens

Fig. 3 Typical *P-s* curves for steel-RAC composite columns

significant difference is that there is no obvious ascent section, which means that the push-out load starts with a decrease phase when the slip is little. For RACFST specimens, this phenomenon is common near the peak point in *P-s* curves. It can be explained that the interface bond damage between steels and RAC develops and accumulates from the loading end to the free end with increasing of slip, so that the load at the free end drops off very quickly.

- Regardless of the SRRAC or RACFST columns, the development of slip at the loading end is earlier than that at the free end, and the shapes of two sides of curves have a certain degree of similarity for each type of composite columns.

3.2 Test process

3.2.1 Test phenomena of SRRAC

In the push-out test, the failure development process can be described with respect to the load-slip curves of SRRAC columns. At the micro-slip stage, the load is small and no obvious slip occurs both at the loading end and the free end of the shape steel, i.e., the load versus slip curve remains linear. With the test keep going, initial slips turned up at the loading end. Almost at the same time, macroscopic cracks started to appear at the surface of free end, and they were parallel to the steel flange. At the internal cracking stage, when the load increased towards a critical value, the free end of the shape steel began to slip, which demonstrated that the adhesion force at the anchorage had nearly been exhausted. After this stage, the rate of the slip began to increase and the ascending portion of the curve became distinctly nonlinear. Later, the cracks gradually developed to the loading end, with the increasing width of them. Near the load reached the peak load, the first crack turned into the main crack throughout the entire length of specimens. At the push-out stage, some longitudinal splitting cracks were developed along the weakest area of the concrete covering. After this stage, the load declined rapidly and the slip increased until the shape steel was completely pushed out. The final failure patterns and crack development pictures of eleven SRRAC columns are shown in Fig. 4.

3.2.2 Test phenomenon of RACFST

Compared with SRRAC columns, because the concrete was filled in the steel tube, there were no cracks appeared in the push-out test. The development of slips in RACFST columns was similar to that in the SRRAC columns, which means that slips also turned up from the loading end to the free end. However, it is worth noting that there was arising a sound of “da, da, da” in the stage of reaching the peak load. It can be explained that the bond force becomes invalid because of the destruction of chemical bond strength, followed by the mechanical biting strength playing a role. It is the sound that the rough places of internal steel tube wall hit the interlaced face of concrete. No crushing on the concrete surface at the loading end and no drummed shape on the steel tube were seen after the test. The final modes of two cross-section types of RACFST are pictured in Fig. 5.

3.3 Bond strength

Currently, there is no uniform definition of bond strength that is universally accepted. Roeder *et al*. (1999) conducted tests on the bond between circular steel tube and concrete, and defined the bond stress capacity as the average interface stress associated with the initial rigid body slip of the core

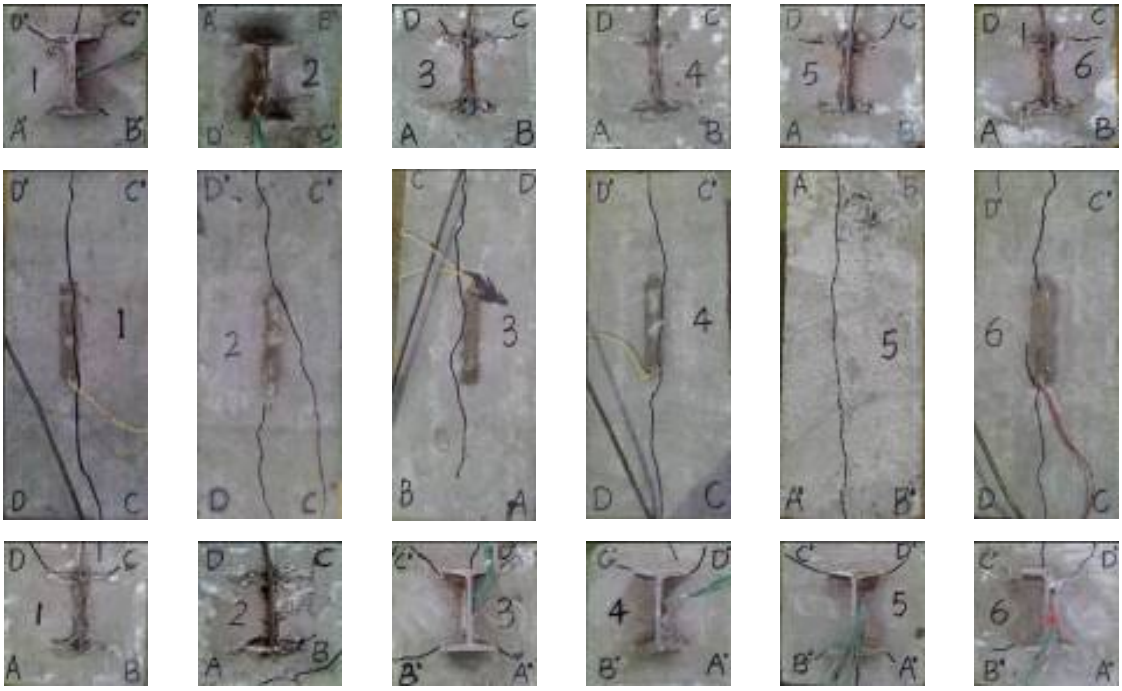

S-RAC-1 S-RAC-2 S-RAC-3 S-RAC-4 S-RAC-5 S-RAC-6

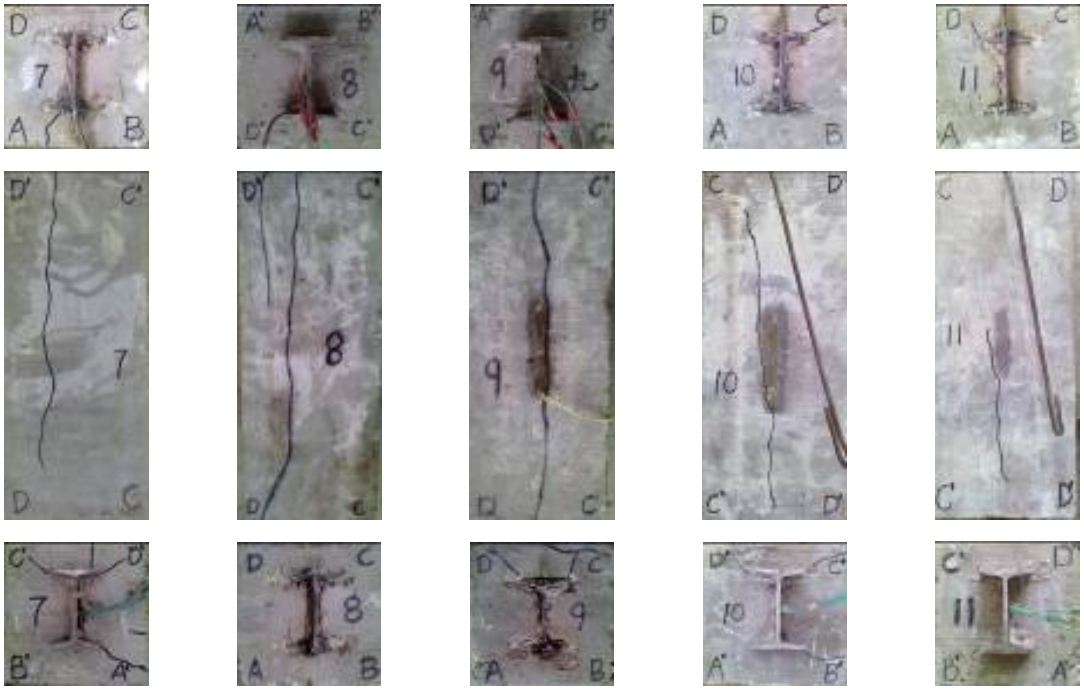

S-RAC-7 S-RAC-8 S-RAC-9 S-RAC-10 S-RAC-11

Fig. 4 Failure models of SRRAC specimens

(a) RACFCST

(b) RACFSST

Fig. 5 Failure models of RACFST specimens

concrete relative to the steel tube. In their tests, there were declining sections on the load-slip curves. In allusion to these kinds of curves, the behavior of concrete was of rigid body motion between the core and the tube with reduced mechanical resistance from interface shear after the slip was greater than that at the peak load. For this reason, maximum average bond stress was used by Shakir-Khalil (1993), Roeder *et al*. (1999), Nezamian *et al*. (2006), De Nardin *et al*. (2007) and Tao *et al*. (2011). On the basis of the above mentioned method, the maximum average bond stress is also adopted in this investigation to represent interfacial ultimate bond strength. The average value of ultimate bond strength (τ_u) was calculated using the following equation

$$\tau_u = P_u / A \tag{1}$$

where, P_u is the peak load in the load-slip curve, which can be called the ultimate push-out load; A is the contact area along the embedment length. The values of τ_u for all the specimens are summarized in Table 4.

3.4 Influence of different parameters

3.4.1 Effect of RCA replacement ratio

The effect of RCA replacement ratio on τ_u is depicted in Fig. 6. In general, the bond strength between shape steel and RAC grows significantly with the increase of RCA replacement ratio, although this development process shows certain volatility at some points of RCA replacement ratios. As shown in Figs. 6(b) and (c), the bond strength under relatively high RCA replacement ratio is lower than that of low RCA replacement ratio of RACFST specimens. As suggested by Butler (2011), there is a generally positive correlation relationship between bond strength and concrete compressive strength. In addition, the RAC compressive strength greatly depends on the water absorption capability and initial cracks of RCA. The phenomenon of bond strength fluctuation can be explained as follows. On the one hand, there exists part of initial micro cracks in the RCA during the process of breaking waste concrete blocks. Compared with NAC, these defects in the concrete may lead to be more brittle. When the loading comes into the nonlinear phase of slip, it can easily cause the mechanical interaction force and frictional force between steel and

RAC drop outworking, so that the bond action can be weaken to a certain extent, which can be called “adverse effect”. On the other hand, the old cement mortar substrate on the surface of RCA owns a high water absorption capacity, which leads to store a part of water in concrete. In the test, for the W/C ratio is kept constant, it is clear that RCA can easily absorb the water from external environment during the process of the casting and nursing of concrete, which can be seen an “internal water curing effect”. To some extent, the result of a foresaid effect can make the concrete strength improved; therefore, it can be called “favorable effect”. In a word, the bond strength is influenced by the above mentioned two effects: when the adverse effect is stronger than the favorable effect, the interfacial bond strength trends to be decrease; or else, it is able to increase. However, the further research and larger data set is required to confirm this phenomenon because of the test limitation.

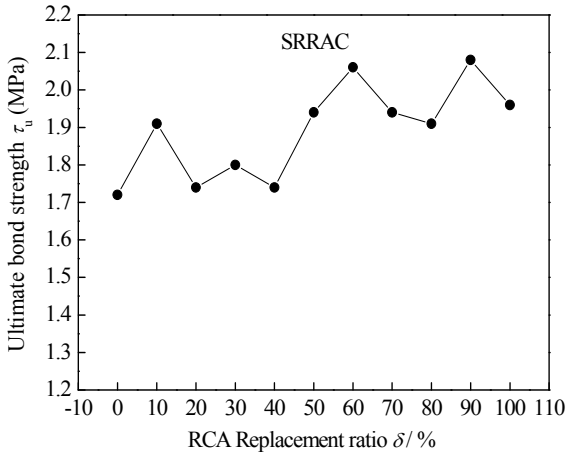

(a) SRRAC

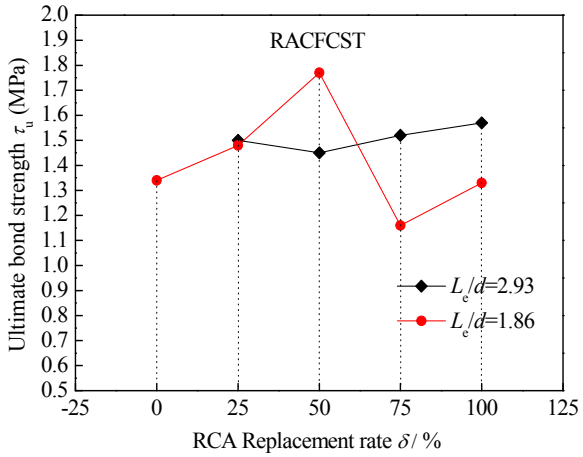

(b) RACFCST

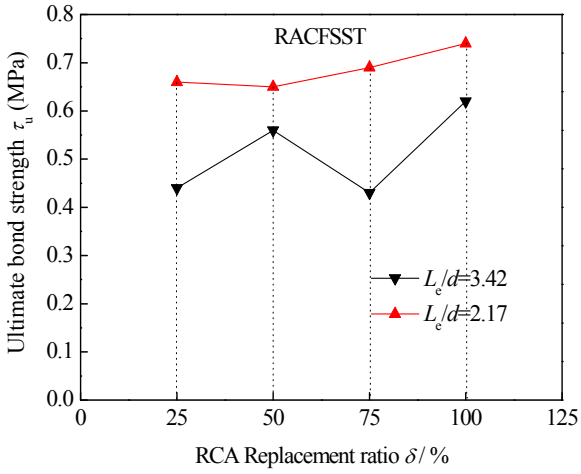

(c) RACFSST

Fig. 6 Effect of RCA replacement ratio on bond strength

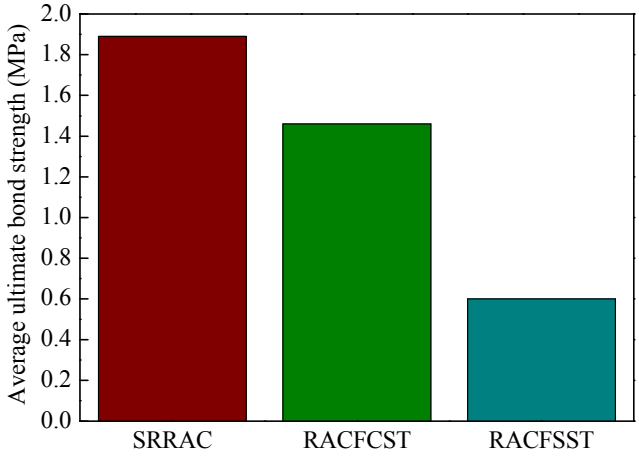

Fig. 7 Effect of steel type and cross-section type on bond strength

3.4.2 Effect of steel type and cross-section type

Due to the different constraint mechanisms, it is no doubt that steel type and cross-section type have impact on the composite action between steel and RAC. Fig. 7 compares the average bond strength among SRRAC specimens, RACFCST specimens and RACFSST specimens. Although the concrete type of SRRAC columns (C30) was lower than that of RACFST columns (C50), it can be clearly seen that the former had much higher bond strength than the latter, and the bond strength of RACFCST columns was twice higher than that of RACFSST columns. These can be explained by the aforesaid different bond mechanisms for the combination type of steel and concrete, i.e., the shape steel embedded in the concrete confined with stirrups are much more effective in transferring the interface shear stress, however, the steel tube surrounding the internal concrete is hard to resist interfacial shear. This means that the confinement effect of shape steel in SRRAC columns is the passive restraint, while the confinement effect of steel tube in RACFST columns is the active constraint. For SRRAC specimens, the shape steel is not only restrained by the external RAC, but also surrounded by the steel reinforcement cage skeleton. These two kinds of constraint systems have the function of joint strengthening for the internal steel. What's more, the RAC has the characteristic of chemical shrinkage in the process of hydration reaction, so that it may lead to be tight in the interface. While for RACFST specimens, the interfacial constraint mechanism is just on the contrary compared with SRRAC.

It can also be found from Fig. 7 that τ_u of RACFCST specimens is much larger than that of RACFSST specimens. This is also owing to the fact that the interface stress mechanism is discrepant on the circular steel tube and square steel tube. For RACFSST specimens, when the loads acting on the core RAC at the loading end, it can cause the concrete expand outwards, therefore, the steel wall can be extruded accordingly. Because of non-radial symmetry of the cross-section of square steel tube, the corners of rectangular cross section have much greater constraint ability to the RAC than the steel plates. The result of interface contacting behavior is that the steel plate trends to separate from the core RAC, which can be called "thin-plate bending effect". While for RACFCST specimens, due to the circular cross-section, their steel plates must be bound when they are pushed along the radial. Therefore, the constraint mechanism is the key leading factor to affect the bond strength between steels and RAC.

3.4.3 Effect of concrete type

Two types of concrete, i.e., HSRAC (C50) and LSRAC (C30), were used in the current test program for RACFSST columns. The effect of concrete type on τ_u can be found in Table 4, where columns of S-RAC-29 and S-RAC-31 are the contrast specimens. It seems that the HSRAC of S-RAC-29 (0.69 MPa) owns higher bond strength than the LSRAC of S-RAC-31 (0.61 MPa). This is consistent with the observation made by Virdi and Dowling (1980) in natural aggregate concrete (NAC). Therefore, although with some limitations of the tests, one conclusion can be conducted that the higher the RAC strength, the larger the bond strength between square steel tube and RAC.

3.4.4 Effect of length-diameter ratio

The relationship between τ_u and length-diameter ratio L_e/D is shown in Figs. 6(b) and (c) for RACFST. For square columns, the trend is that the τ_u decreased with the increase of L_e/D. But the trend for circular columns is just at the opposite, except the point of RCA replacement ratio δ = 50%. Since the bond strength is mainly provided by the steel tube wall-concrete interaction near the loading end and the constraint ability is relatively poor for square columns, the average bond strength decreases if the interface embedment length increases. Compared with square steel tubes, the bond stress distributes more evenly along the embedment length of circular steel tubes due to the completely symmetrical section form. This can be explained that the circular steel tubes have good constraint ability to the core concrete. In a word, the longer the column, the higher the tolerance of surface irregularities and overall imperfections are.

4. Bond strength calculation and comparison

Due to the difference of materials used, the existing calculation formulas about the bond strength between steels and concrete (S-C) are limited to the NAC. This means that the suitable computing methods for the bond strength between steels and RAC have been a situation of short of knowledge. In order to demonstrate that the available calculation modes of S-C are suitable for steel-RAC or not, the bond strength between steels and RAC of steel-RAC specimens are calculated via using the following eight models. The calculation results are listed in Table 5.

4.1 Bond strength in SRRAC

Li *et al*. (1993) proposed a formula based on the fitted test results as follows, where the thickness of concrete covering, concrete type, shape steel section height and transverse stirrup ratio were taken into consideration.

$$\tau_u^c = (0.1696 + 0.0846C_{ss}/h + 57.43\rho_{sv})f_t \tag{2}$$

Yang (2003) put forward an expression which focuses on the parameters of the thickness of concrete covering, concrete type, and diameter of reinforcing steel bar and embedded length of shape steel.

$$\tau_u^c = (0.2921 + 0.4593C_{ss}/d - 0.00781L_e/d)f_t \tag{3}$$

Deng (2004) gathered the above parameters and proposed a modified the formula below.

$$\tau_u^c = 0.0827f_t + 0.0874\rho_{sv} + 0.8624C_{ss}/h - 0.0454L_e/h) + 0.0034 \tag{4}$$

where, C_{ss} is the thickness of concrete cover, h is the height of shape steel section, d is the diameter of reinforcement steel bar, ρ_{sv} is the transverse stirrup ratio, L_e is the embedded length of shape steel. f_t is the axial tensile strength of concrete, and this value can be conversed through the axial compressive strength (f_{cu}) in accordance with Chinese Code for the design of reinforced concrete structures (GB50010) (2010).

4.2 Bond strength in RACFCST

Considering the constraint conditions of circle steel tube (its external diameter D and wall thickness t), Brett *et al*. (2008) provided a calculation formula as follows

$$\tau_u^c = 2.109 - 0.026(D/t) \tag{5}$$

Cai (2003) regarded the concrete strength as the main factor to affect the bond strength between steel and concrete

$$\tau_u^c = 0.1(f_{cu})^{0.4} \tag{6}$$

where f_{cu} is the cube compressive strength of concrete, and it is limited to the concrete type from C40 to C80. For the NAC, the calculation expression is no longer applicable when the concrete type is C30. While for the RAC, there is a big difference that the concrete strength in a specific range can be improved with a constant designing water-cement ratio, compared with NAC. This means that the request of concrete type can be relaxed.

Based on the test parameters, Kang (2008) fitted the following bond strength calculation expression.

$$\tau_u^c = \frac{1}{\gamma} k \left[\left(-0.00028 \left(\frac{4L_e}{D} \right) + 0.11121 \left(\frac{D}{t} \right) + 29.09049\,\alpha + 0.034390\,\theta - 7.36037 \right) f_t \right] \tag{7}$$

where γ is the correction coefficient influenced by uncertain factors, and its value is advised to be 0.96. k is the surface condition influence coefficient of steel tube, and in this study, its value is advised to be 1.3 without derusting process in steel tube. α is the cross-sectional steel ratio of concrete-filled circle steel tube (CFCST). L_e is the interface embedment length. θ ($\theta = A_s f_y / (A_c f_c)$) is the confinement coefficient of CFCST member, A_s is the cross-sectional area of circular steel tube, f_y is the yield strength of circular steel tube, A_c is the cross-sectional area of core RAC, f_c is the compressive strength of concrete prism. f_t is the axial tensile strength of concrete.

4.3 Bond strength in RACFSST

Yang and Han (2006) put forward a calculation model involving the concrete type, cross-section dimension, length-diameter ratio. And the expression is shown as follows.

$$\tau_u^c = p \cdot (0.00268 f_{cu} + 0.3) \cdot f(\beta) \cdot f(\lambda) \cdot f(D/t) \tag{8}$$

$$f(\beta) = 1.28 - 0.28\beta \tag{9}$$

$$f(\lambda) = 1.36 - 0.09 \ln \lambda \tag{10}$$

$$f(D/t) = 1.35 - 0.09\ln(D/t) \tag{11}$$

$$\beta = D/B, \quad \lambda = L_e/B \tag{12}$$

where D is the long side length of square steel tube; B is the short side length of square steel tube; t

Table 4 Test results and values of calculation models

Computation model		S-RAC-1	S-RAC-2	S-RAC-3	S-RAC-4	S-RAC-5	S-RAC-6	S-RAC-7	S-RAC-8	S-RAC-9	S-RAC-10	S-RAC-11
Test value	τ_u	1.72	1.91	1.74	1.79	1.74	1.94	2.06	1.94	1.91	2.08	1.96
Li model	τ_u^c	1.11	1.16	1.19	1.16	1.27	1.26	1.3	1.39	1.46	1.38	1.35
	τ_u^c / τ_u	0.64	0.61	0.69	0.65	0.73	0.65	0.63	0.72	0.75	0.67	0.69
Yang model	τ_u^c	1.84	1.93	1.99	1.93	2.09	2.08	2.16	2.31	2.34	2.29	2.25
	τ_u^c / τ_u	1.07	1.01	1.14	1.07	1.21	1.07	1.05	1.19	1.25	1.1	1.14
Deng model	τ_u^c	1.55	1.57	1.58	1.57	1.59	1.59	1.61	1.63	1.64	1.63	1.62
	τ_u^c / τ_u	0.89	0.82	0.91	0.87	0.92	0.82	0.78	0.84	0.86	0.78	0.83

Computation model		S-RAC-13	S-RAC-14	S-RAC-15	S-RAC-16	S-RAC-17	S-RAC-18	S-RAC-19	S-RAC-20	S-RAC-21
Test value	τ_u	1.5	1.45	1.52	1.57	1.34	1.48	1.77	1.16	1.33
Brett model	τ_u^c	1.99	1.99	1.99	1.99	1.99	1.99	1.99	1.99	1.99
	τ_u^c / τ_u	1.33	1.37	1.31	1.27	1.48	1.34	1.12	1.71	1.49
Cai model	τ_u^c	0.51	0.51	0.50	0.49	0.51	0.51	0.51	0.50	0.50
	τ_u^c / τ_u	0.34	0.35	0.33	0.31	0.38	0.34	0.29	0.43	0.38
Kang model	τ_u^c	2.75	2.7	2.68	2.64	2.73	2.75	2.71	2.68	2.65
	τ_u^c / τ_u	1.83	1.86	1.76	1.68	2.04	1.86	1.53	2.31	1.99

Computation model		S-RAC-22	S-RAC-23	S-RAC-24	S-RAC-25	S-RAC-27	S-RAC-28	S-RAC-29	S-RAC-30	S-RAC-31
Test value	τ_u	0.44	0.56	0.43	0.62	0.66	0.65	0.69	0.74	0.61
Yang model	τ_u^c	0.58	0.58	0.58	0.57	0.6	0.59	0.59	0.59	0.54
	τ_u^c / τ_u	1.32	1.04	1.35	0.92	0.91	0.91	0.86	0.80	0.89
Zhao model	τ_u^c	-0.3	-0.3	-0.3	-0.3	0.12	0.12	0.12	0.12	0.12
	τ_u^c / τ_u	-0.68	-0.54	-0.70	-0.48	0.18	0.18	0.17	0.16	0.20

*Note: τ_u^c is standing for the computed result under each calculation model

is the wall thickness of square steel tube; L_e is the interface embedment length. $\alpha = 0.6$ and $p = 1.0$ are advised in Yang's research report.

Zhao and Liu (2011) summarized the study foundations of the predecessors, and then extracted a reference model for bond strength between square steel tube and concrete.

$$\tau_u^c = (\alpha / \beta)(2 - 0.0298B/t - 0.32L_e/B) \tag{13}$$

where α is the surface coefficient for square steel tube, and its value is 1.3 in this study. β is the security coefficient, and the suggested value is 1.26. B is the exterior length of square steel tube; t is the wall thickness of square steel tube; L_e is the interface embedment length.

4.4 Discussion

Table 4 summarizes different computed bond strengths for steel-RAC columns in different suggested design formulas. From the comparison shown in Table 4, it is conservative to use the computational models of Li *et al*. (1993), Deng (2004) and Cai (2003), however, the test values are much larger than the results adopting the formulas of Yang, Brett and Kang. In addition, it is worth noting that there are some bounded nesses when using those suggested models for concrete-filled square steel tube. With regard to using the model of Yang, the calculated values are larger than the test results if the RCA replacement ratio is relatively small and length-diameter ratio is comparatively large, if not, it may be safe to compute the bond strength. Also, the results from Zhao's model (Zhao *et al*. 2009) are not suitable for calculating the bond strength of RACFSST, because the real bond strength cannot be the negative value. In view of this, with the limitation of the current tests, it is suggested that it needs to be cautious when using these models to design steel-RAC composite structures.

5. Bond shear transmission length

It should be made clearly that the mechanisms of bond shear transmission length both at the column foot and the anchorage zone of beam-column joint. This means that it is helpful for the engineers to understand how and where to set strengthen area in order to effectively transfer the internal force at these locations. In this study, the bond shear transmission length between steels and RAC was investigated by the way of mechanical derivation. The analysis process of this length is shown below.

After the interface bond stress experiences a shear transfer length, both the strains of steel and RAC tend to be equal. Thus, these two strains keep a state of strain coordination in the rest interfacial length along the embedment length range. According to the equilibrium principle of longitudinal force between steels and RAC, the equilibrium equations can be expressed as follows.

For SRRAC

$$P = P_c + P_s + P_{sb} \tag{14a}$$

For RACFST

$$P = P_c + P_s \tag{14b}$$

The Eq.(14a) can be modified as the formula $P = A_c \cdot E_c \cdot \varepsilon_{c,x} + A_s \cdot E_s \cdot \varepsilon_{s,x} + A_{sb} \cdot E_{sb} \cdot \varepsilon_{sb,x}$, where, in the push-out test, the strain of construction longitudinal reinforcement keeps strain coordination

to the RAC strain, and that is to say that $\varepsilon_{s,x}=\varepsilon_{sb,x}$.

Therefore

$$P = A_c E_c[(1+n_1\omega_1)\varepsilon_{c,x} + n_2\omega_2\varepsilon_{c,x}] \tag{15a}$$

$$P = A_c E_c\varepsilon_{c,x} + A_s E_s\varepsilon_{s,x} = A_c E_c(\varepsilon_{c,x} + n_2\omega_2\varepsilon_{s,x}) \tag{15b}$$

Because of the relationship $\varepsilon_{c,x}=\varepsilon_{s,x}=\varepsilon_{sb,x}$, thus the strain representative parameter ε can be calculated as

$$\varepsilon = P/[A_c E_c(1+n_1\omega_1+n_2\omega_2)] \tag{16a}$$

$$\varepsilon = P/[A_c E_c(1+n_2\omega_2)] \tag{16b}$$

By analyzing the isolated shape steel in SRRAC and isolated core concrete in RACFST, their force equilibrium equations are constructed, respectively.

$$P_s = \int_0^{l_t}\tau(x)\cdot c dx = A_s E_s\varepsilon = P\Big/\Big[(1+n_1\omega_1+n_2\omega_2)\times(n_2\omega_2)^{-1}\Big] \tag{17a}$$

$$P_c = \int_0^{l_t}\tau(x)\cdot c dx = A_c E_c\varepsilon = P/(1+n_2\omega_2) \tag{17b}$$

In the push-out test, the bond stress between steels and RAC can uniformly distribute along the interface embedment length when the bond failure occurs, and that is to say that the bond strength in any point along the embedment length $\tau(x)$ reaches the largest bond stress $\tau_{\max}$. Hence, the value of $\tau_{\max}$ can be determined by the test result that $\tau(x)$ approximately equal to the average ultimate bond strength τ_u. In this way, the bond shear transmission length l_t is expressed as:

For SRRAC

$$l_t = P_u\Big/\Big[(1+n_1\omega_1+n_2\omega_2)\cdot c\cdot\tau_u\cdot(n_2\omega_2)^{-1}\Big] \tag{18a}$$

For RACFST

$$l_t = P_u\Big/\Big[(1+n_2\omega_2)\cdot c\cdot\tau_u\Big] \tag{18b}$$

where P is the external force, and in this investigation, P is the push-out load; P_c is the pressure of RAC, P_s is the pressure of steel (shape steel or steel tube) and P_{sb} is the pressure of longitudinal reinforcing steel bars. A_c is the compression area of RAC; A_s is the cross-sectional area of shape steel or steel tube; A_{sb} is the cross-sectional area of longitudinal reinforcing steel bars. E_c is the elastic modulus of RAC, whose value can be computed through the expression of Chinese standard GB 500010-2010; E_s is the elastic modulus of shape steel or steel tube; E_{sb} is the elastic modulus of longitudinal reinforcing steel bars. $\varepsilon_{c,x}$, $\varepsilon_{s,x}$ and $\varepsilon_{sb,x}$ are the strains of RAC, shape steel or steel tube and longitudinal reinforcing steel bars along the interfacial embedment length, respectively. c is the section perimeter of shape steel or the inside edge perimeter of steel tube section. The coefficients n_1, ω_1, n_2 and ω_2 are expressed as $n_1=E_{sb}/E_c$, $\omega_1=A_{sb}/A_c$, $n_2=E_s/E_c$, $\omega_2=A_s/A_c$.

Table 5 shows the bond shear transmission length of each specimen. It can be seen from Table 5 that the bond shear transmission length between steels and RAC changes with the steel type. On average, the mean values l_t of SRRAC columns, RACFCST columns and RACFSST columns are

Table 5 Bond shear transmission length of specimens

Specimen code	l_t (mm)	Specimen code	l_t (mm)	Specimen code	l_t (mm)
S-RAC-1	85.35	S-RAC-11	81.57	S-RAC-22	217.46
S-RAC-2	83.95	S-RAC-13	204.21	S-RAC-23	217.81
S-RAC-3	83.56	S-RAC-14	202.27	S-RAC-24	198.48
S-RAC-4	84.14	S-RAC-15	202.16	S-RAC-25	199.32
S-RAC-5	82.43	S-RAC-16	201.62	S-RAC-27	128.58
S-RAC-6	82.71	S-RAC-17	128.44	S-RAC-28	127.81
S-RAC-7	82.03	S-RAC-18	129.46	S-RAC-29	126.58
S-RAC-8	80.95	S-RAC-19	128.64	S-RAC-30	126.45
S-RAC-9	80.22	S-RAC-20	128.11	S-RAC-31	117.85
S-RAC-10	81.03	S-RAC-21	127.57		

82.54 mm, 202.57 mm ($L_e/D=2.93$) and 128.45 mm ($L_e/D=1.86$), 208.27 mm ($L_e/D=3.42$) and 125.45 mm ($L_e/D=2.17$), respectively. In general, the transmission length of SRRAC is much smaller than that of RACFST. For the larger length-diameter ratio, the bond shear transmission length of RACFSST (208.27 mm) on average is larger than that of the RACFCST (202.57 mm), although the length-diameter ratio of the former is bigger than the latter's (L_e/D=3.42 for RACFSST and 2.93 for RACFCST). While under the conditions of the shorter length-diameter ratio of RACFST, the values of circular specimens do not appear to be much different from the square specimens. Hence, it is thus clear that different constraint mechanisms of steel-RAC specimens lead to the changes of interface bond shear transmission lengths.

6. Conclusions

An experimental program of bond characteristics between steels and recycled aggregate concrete, including steel reinforced recycled aggregate concrete columns, recycled aggregate concrete-filled circular steel tube columns and recycled aggregate concrete-filled square steel tube columns, is discussed in this paper. The following conclusions can be drawn based on the results of this investigation.

- Load-slip curves of SRRAC, RACFCST and RACFSST specimens were different from each other in their shapes; it means that different types of steels and RAC have respective mechanical characteristics in the bond action. The initial slip of all the specimens at the loading end develops earlier than that at the free end.
- By comparing the average ultimate bond strengths of three steel types of specimens, the value of SRRAC columns is larger than that of RACFST, and the value of circular specimens is higher than that of the square specimens. It reveals that the effect of passive restraint for SRRAC is superior to the active constraint of RACFST in aspect of steel embedment way; in addition, the circular cross-section steel tube has a better uniform constraint effect on the core RAC than the square steel tube.
- Due to the large water absorption capability of old cement mortar substrate and initial cracks in RCA, the bond strength of steel-RAC columns generally behaves a fluctuation on rising

with the increase of RCA replacement ratio. More research is needed for these columns with finely-divided RCA replacement ratios.

- Within the limitations of the tests, the higher the RAC strength, the larger the bond strength between square steel tube and RAC. The bond strength of RACFSST columns decreased with increasing of L_e / D, while the longer the RACFCST columns, the higher the tolerance of surface irregularities and overall imperfections are.
- Within the limitation of existing practical calculation models of bond strength of steel-RAC, they are needed to be reasonably used when designing steel-RAC composite structures.
- A strong relationship was found between bond shear transmission length and bond strength for the anchorage area in steel-RAC composite structures. The average length order of these three types of steel-RAC columns is arranged below: RACFSST l_t > RACFCST l_t > SRRAC l_t. The results show that the interfacial constraint mechanisms for SRRAC, RACFCST and RACFSST become weak in turn.
- Based on the research results reported in this study, it seems that the RAC has significant influence on the ultimate bond strength. To carry out an accurate bond damage analysis for considering the effect of RCA content in concrete, further research is needed to put forward a suitable bond stress-slip model within a damage factor. The experimental work presented in this investigation has provided a good basis for developing this model.

Acknowledgments

The presented research is conducted under the financial support of the Natural Science Foundation of China (No: 50908057 and 51268004), the Guangxi Natural Science Foundation (No: 2012GXNSFAA053203 and 2013GXNSFDA019025), the Guangxi Science and Technology Key Project (No: 12118023-3), the Key Project of Guangxi Science and Technology Lab Center (No: LGZX201102) and Innovation Project of Guangxi Graduate Education (No: YCBZ2012005).

References

Brett, C.G., Cenk, T., Jerome, F.H. and Paul, H.S. (2008), *A Synopsis of Studies of the Monotonic and Cyclic Behavior of Concrete-Filled Steel Tube Beam-Columns*: *Structural Engineering Report*, Department of Civil and Environmental Engineering, University of Illinois at Urbana Champaign, Urbana, IL, USA.

Butler, L., West, J.S. and Tighe, S.L. (2011), "The effect of recycled concrete aggregate properties on the bond strength between RCA concrete and steel reinforcement", *Cement Concrete Res*., **41**(10), 1037-1049.

Cai, S.H. (2003), *Modern Times Structures of Concrete Filled Steel Tube*, China Communications Press, Beijing, China. [In Chinese]

Chen, Z.P., Zhang, X.G., Zhang, S.Q. and Xue, J.Y. (2011), "Experimental study on axial compressive behaviors of steel recycled concrete composite columns", *Adv*. *Mater*. *Res*., **243-249**, 1242-1247.

De Juan, M.S. and Gutiérrez, P.A. (2009), "Study on the influence of attached mortar content on the properties of recycled concrete aggregate", *Construct*. *Build*. *Mater*., **23**(2), 872-877.

De Nardin, S. and El Debs, A.L.H.C. (2007), "Shear transfer mechanisms in composite columns: an experimental study", *Steel Compos*. *Struct*., *Int*. *J*., **7**(5), 377-390.

Deng, G.Z. (2004), "Experimental study on and basic theory analysis on bond-slip behavior between shape steel and concrete in steel reinforced concrete structures", Xi'an University of Architecture and Technology, Xi'an, China. [In Chinese]

Gholamreza, F., Razaqpur, A.G., Isgor, O.B., Abbas, A., Fournier, B. and Foo, S. (2012), "Bond perfor-

mance of deformed steel bars in concrete produced with coarse recycled concret eaggregate", *Can. J. Civil Eng.*, **39**(2), 128-139.
Hansen, T.C. (1992), *Recycling of Demolished Concrete and Masonry*, Londom, E&FN SPON.
Huang, Y.J., Xiao, J.Z. and Zhang, Ch. (2012), "Theoretical study on mechanical behavior of steel confined recycled aggregate concrete", *J. Construct. Steel Res.*, **76**(12), 100-111.
Kang, X.L. (2008), *Study on Compositing Mechanical Performance and Bond-Slip Performance of Concrete Filled Steel Tube*, Xi'an University of Architecture and Technology, Xi'an, China. [In Chinese]
Konno, K., Yasuhiko, S., Yoshio, K. and Msaji, O. (1997), "Property of recycled concrete column encased by steel tube subjected to axial compression", *Transactions of the Japan Concrete Institute*, **19**(2), 231-238.
Li, H., An, J.L. and Jiang, W.S. (1993), "An experimental investigation on bond behavior between steel and concrete", *J. Harbin Inst. Tech.*, **26**(Suppl), 214-223. [In Chinese]
Liu, C., Zhu, B.J. and Shi, Y.L. (2011), "Coseismic stress variation and numerical analysis of 2011 Japan–Honshu 9.0 earthquake", *Theor. Appl. Fract. Mech.*, **55**(2), 118-130.
Liu, Y.X., Zha, X.X. and Gong, G.B. (2012), "Study on recycled-concrete-filled steel tube and recycled concrete based on damage mechanics", *J. Construct. Steel Res.*, **71**(4), 143-148.
Michael, D. and Li, L. (2011), "Earthquake reconstruction in Wenchuan: Assessing the state overall planand addressing the 'forgotten phase'", *Appl. Geograph.*, **31**(3), 998-1009.
Nandasena, N.A.K., Sasaki, Y. and Tanaka, N. (2012), "Modeling field observations of the 2011 Great East Japan tsunami: Efficacy of artificial and natural structures on tsunami mitigation", *Coast. Eng.*, **67**(12), 1-13.
Nezamian, A., Al-Mahaidi, R. and Grundy, P. (2006), "Bond strength of concrete plugs embedded in tubular steel piles under cyclic loading", *Can. J. Civil Eng.*, **33**(2), 111-125.
Nixon, P.J. (1978), "Recycled concrete as an aggregate for concrete – A review", *Mater. Struct.*, **11**(5), 371-378.
Qin, W.Y., Chen, Y.L. and Chen, Z.P. (2012), "Experimental study on flexural behaviors of steel reinforced recycled coarse aggregate concrete beams", *Appl. Mech. Mater.*, **166-169**, 1614-1619.
Roeder, C., Cameron, B. and Brown, C. (1999), "Composite action in concrete filled tubes", *ASCEJournal of Structural Engineering*, **125**(5), 477-484.
Shakir-Kalil, H. (1993), "Resistance of concrete-filled steel tubes to pushout forces", *Struct. Eng.*, **71**(13), 234-243.
Takewaki, I., Murakami, S., Fujita, K., Yoshitomi, S. and Tsuji, M. (2011), "The 2011 off the Pacific coast of Tohoku earthquake and response of high-rise buildings under long-period ground motions", *Soil Dyn. Earthq. Eng.*, **31**(11), 1511-1528.
Tao, Z., Han, L.H., Brian, U. and Chen, X. (2011), "Post-fire bond between the steel tube and concrete in concrete-filled steel tubular columns", *J. Construct. Steel Res.*, **67**(3), 484-496.
Virdi, K.S. and Dowling, P.J. (1980), "Bond structure in concrete filled steel tubes", *IABSE Proceedings P-33/80*, 125-139.
Xiao, J.Z. and Falkner, H. (2007), "Bond behaviour between recycled aggregate concrete and steel rebars", *Construct. Build. Mater.*, **21**(2), 395-401.
Xiao, J., Li, J. and Zhang, Ch. (2005), "Mechanical properties of recycled aggregate concrete under uniaxial loading", *Cement Concrete Res.*, **35**(6), 1187-1194.
Yang, Y. (2003), *Study on the Basic Theory and its Application of Bond-Slip between Shape Steel and Concrete in SRC Structures*, Xi'an University of Architecture and Technology, Xi'an, China. [in Chinese].
Yang, Y.F. and Han, L.H. (2006), "Experimental behaviour of recycled aggregate concrete filled steel tubular columns", *J. Construct. Steel Res.*, **62**(12), 1310-1324.
Yang, Y.F. and Han, L.H. (2006), "Research on bond behavior between steel and concrete of self-compacting concrete filled steel tubes with rectangular sections", *Indust. Construct.*, **36**(11), 32-36. [In Chinese]
Zhao, Y.C. and Liu, J. (2011), "The compute method of concrete filled square steel tube bond stress", *Sci.*

Tech. *Information*, **5**, 321-313. [In Chinese]
Zhao, B., Taucer, F. and Rossetto, T. (2009), "Field investigation on the performance of building structures during the 12 May2008 Wenchuan earthquake in China", *Eng*. *Struct*., **31**(8), 1707-1723.

CC